Published in final edited form as:
J Mol Cell Cardiol. 2011 September ; 51(3): 409–418. doi:10.1016/j.yjmcc.2011.06.001.

Myosin Cross-Bridges Do Not Form Precise Rigor Bonds in Hypertrophic Heart Muscle Carrying Troponin T Mutations

K. Midde[1], **V. Dumka**[1], **J.R. Pinto**[4], **P. Muthu**[4], **P. Marandos**[3], **I. Gryczynski**[1,2], **Z. Gryczynski**[1,3], **J.D. Potter**[4], and **J. Borejdo**[1]

[1]Dept of Molecular Biology & Immunology and Center for Commercialization of Fluorescence Technologies, University of North Texas, Health Science Center, 3500 Camp Bowie Blvd, Fort Worth, TX 76107

[2]Dept of Cell Biology and Genetics and Center for Commercialization of Fluorescence Technologies, University of North Texas, Health Science Center, 3500 Camp Bowie Blvd, Fort Worth, TX 76107

[3]Dept of Physics and Astronomy, Texas Christian University, 2800 S. University Dr., Fort Worth, Texas 76129

[4]Department of Molecular and Cellular Pharmacology, University of Miami, Miller School of Medicine, Miami, FL33136

Abstract

Distribution of orientations of myosin was examined in *ex-vivo* myofibrils from hearts of transgenic (Tg) mice expressing Familial Hypertrophic Cardiomyopathy (FHC) troponin T (TnT) mutations I79N, F110I and R278C. Humans are heterozygous for sarcomeric FHC mutations and so hypertrophic myocardium contains a mixture of the wild-type (WT) and mutated (MUT) TnT. If mutations are expressed at a low level there may not be a significant change in the global properties of heart muscle. In contrast, measurements from a few molecules avoid averaging inherent in the global measurements. It is thus important to examine the properties of only a few molecules of muscle. To this end, the lever arm of one out of every 60,000 myosin molecules was labeled with a fluorescent dye and a small volume within the A-band (~1 fL) was observed by confocal microscopy. This volume contained on average 5 fluorescent myosin molecules. The lever arm assumes different orientations reflecting different stages of acto-myosin enzymatic cycle. We measured the distribution of these orientations by recording polarization of fluorescent light emitted by myosin-bound fluorophore during rigor and contraction. The distribution of orientations of rigor WT and MUT myofibrils were significantly different. There was a large difference in the width and of skewness and kurtosis of rigor distributions. These findings suggest that the hypertrophic phenotype associated with the TnT mutations can be characterized by a significant increase in disorder of rigor cross-bridges.

*corresponding author tel 817 735 2106, fax 817 735 2118, Julian.Borejdo@unthsc.edu.
K.Midde and V. Dumka contributed equally to this paper.

DISCLOSURES:
None

Keywords

Cardiac Hypertrophy; Troponin T; polarization of fluorescence; confocal microscopy

Muscle contraction results from ATP-coupled interactions of myosin cross-bridges with actin filaments. These interactions involve series of conformational changes of the myosin lever arm which result in the development of the contractile force. The conformational changes involve unwinding of the “kink” in the relay helix of the converter domain of the myosin head that lead to the rotation of the converter domain (power-stroke; [1]. The result is the angular change of the myosin lever arm [1–4]. We have used these angular changes to characterize the properties of cardiac muscle. We report that the distribution of angular changes is very different in rigor muscle of the healthy and hypertrophic hearts carrying troponin T (TnT) mutations.

Familial Hypertrophic Cardiomyopathy (FHC) is believed to be caused by mutations in sarcomeric proteins of the heart. In this report we have focused on mutations in the ventricular TnT [5, 6]. Tn and Tm mutations often alter Ca^{2+} sensitivity of contractility. In the heart, severity of familial hypertrophic cardiomyopathy is related to the degree to which Ca^{2+} sensitivity is increased by mutations [7, 8]. Mutations in other subunits of Tn have been extensively investigated e.g. [9]. TnT mutations are often associated with malignant outcomes [10]. In this paper we carried out measurements using single molecule detection (SMD). The rationale for SMD measurements is that humans are heterozygous for FHC. It follows that hypertrophic myocardium contains a mixture of the wild-type and mutated proteins. If the degree of expression of mutated protein is small, only a small fraction of myosins interact with actin that carries mutated TnT. In such muscles, it is possible that averaging over billions of molecules inherent in global measurements such as tension, ATPase or Ca sensitivity, will not reveal differences between mutated and wild type muscle (while in some cases only 10 % expression is sufficient to reveal differences in global properties [11], the particular mutation examined in this case, R145W in troponin I, was associated with restrictive cardiomyopathy which is more severe than FHC mutations examined here. Severity may be associated with cooperativity, i.e. mutation of one TnI molecule may affect neighboring molecules or with the fact that mutations at residue 145 of cTnI are particularly sensitive indicator of disease - even two different aa replacements at this residue are associated with completely different cardiomyopathies). In contrast, if only a few molecules of myosin are observed, there is no averaging of responses from a large number of molecules and there is a good chance that experiments will reveal hypertrophic behavior. We have therefore worked in mesoscopic regime where fluctuations from the average are significant [12]. We compared the distribution of orientations (polarized fluorescence) of ~5 myosin molecules of the healthy and diseased hearts.

Fig. 1 illustrates rationale behind the method used to collect the data. Myosin light chain 1 (LC1) is labeled with rhodamine and exchanged with native LC1 of a myofibril (MF). A small volume within the A-band is illuminated by the laser beam focused to the diffraction limit (green). The fluorescence is observed by a microscope through a small pinhole (confocal detection) so the detector sees only the volume indicated by a dashed line. It is an ellipsoid of revolution whose volume is approximately 1 μm^3. Because myosin is labeled very sparsely (only one of approximately 60,000 myosin molecules carry fluorescent LC1), this detection volume (DV) contains only ~5 fluorescent molecules (see the section “Number of observed molecules” in Results). Myosin cross-bridges in contracting muscle undergo periodic changes of orientation due to power stroke and to association-dissociation from actin, leading to fluctuations in polarized fluorescence of rhodamine. Myosin cross-bridges in rigor muscle do not rotate, but the distribution of orientations reflects on how well

they are organized. Orientations are recorded by measuring parallel (∥) and perpendicular (⊥) components of fluorescent light. The normalized ratio of the difference between these components is called Polarized Fluorescence (PF) and is a sensitive indicator of the orientation of the transition dipole of the fluorophore [2–4, 13–18]. We characterize rigor by the distribution of orientations (a histogram). A histogram is a diagram showing the orientation (PF) on the x-axis and the number of times that a given orientation occurs on the y-axis. Histograms are quantified by their Full Width at Half Maximum (FWHM), by the "velocity" plots (the rate that a given polarization changes) and by a skewness and kurtosis. A positive skewness means that the tail of the curve points towards positive values of the histogram. A positive kurtosis is expressed by long tails and higher peaks compared to the Gaussian curves. A negative skewness means that the tail of the curve points towards negative values of the histogram. A negative kurtosis means that the tails are smaller than those of Gaussian curves.

We report that the distribution of orientations in rigor WT and MUT myofibrils were significantly different. There was large difference in the velocity plots, FWHM and the values of both skewness and kurtosis. These findings suggest that the hypertrophic phenotype associated with the TnT mutations can be characterized by a significant increase in disorder of rigor cross-bridges.

MATERIALS AND METHODS

Chemicals and solutions

Tetramethylrhodamine-5-iodoacetamide dihydroiodide (5-TMRIA) (single isomer) was purchased from Molecular Probes (Eugene, OR, Cat. No. T-6006). All other chemicals were from Sigma-Aldrich (St Louis, MO). The composition of solutions was as in [19]. Briefly: the Ca-rigor solution contained 50 mM KCl, 0.1 mM $CaCl_2$, 10 mM Tris pH 7.5, 1 mM DTT. Contracting solution had the same composition plus 5 mM ATP. Mg^{2+}-rigor solution had the same composition except that 2 mM $MgCl_2$ replaced Ca^{2+}. EDTA-rigor had the same composition except that it did not contain either Mg^{2+} or Ca^{2+} and contained in addition 5 mM EDTA.

FHC-TnT mutations in mice

The degree of the human TnT expression in the Tg mouse hearts were 71%, 52%, 45% and 50% for L3-WT, L8-I79N, L1-F110I and L5-R278C mutations, respectively [5, 6]. The mice were euthanized according to the approved protocol by the animal care and use committee (IACUC) of the Miller School of Medicine University of Miami. After euthanasia, the hearts were immediately frozen and stored at − 80°C until needed. The Tg hearts used in this study were ~ 3 to 7 months-old. The frozen hearts were thawed and then briefly rinsed (no more than 30 s) with ice-cold 0.9% NaCl. Muscle strips from left and right ventricles and papillary muscles were dissected at 4 °C in a cold room in ice-cold pCa 8 solution (10–8 M [Ca^{2+}], 1 mM [Mg^{2+}], 7 mM EGTA, 2.5 mM [$MgATP^{2+}$], 20 mM MOPS, pH 7.0, 15 mM creatine phosphate, ionic strength = 150 mM adjusted with potassium propionate) containing 30 mM BDM and 15% glycerol [19]. After dissection, muscle strips were transferred to pCa 8 solution mixed with 50% glycerol and incubated for 1 h on ice. Then the muscle strips were transferred to fresh pCa 8 solution mixed with 50% glycerol and containing 1% Triton X-100 for 24 h at 4 °C. Muscle strips were finally transferred to a fresh batch of pCa 8 solution mixed 1:1 with glycerol and kept at − 20 °C until used for the preparation of myofibrils.

LC1 Expression

Light Chain 1 expression was done as described previously [20]: Briefly, pQE60 vector containing recombinant LC1 (single cysteine residue) was donated by Dr. Lowey (University of Vermont). The DNA plasmid was transformed into E.coli M15 competent cells and recombinant clones were selected by ampicillin resistance. The clones containing LC1-cDNA insert were confirmed by DNA sequencing (Iowa State University of Science and Technology). LC1 protein was over expressed in Luria broth containing 100 μg/ml of ampicillin by inducing with IPTG. His-tagged LC1 protein was affinity purified on Ni-NTA column. The imidazole eluted fractions were run on SDS-PAGE followed by Western analysis with Anti-LCN1 antibody (Abcam, CA). Fractions containing LC1 were pooled together and dialyzed against buffer containing 50 mM KCl and 10 mM phosphate buffer (pH 7.0). Purified protein showed a single band migrating on SDS-PAGE at ~25-kDa [20].

Preparation of myofibrils

Left or right ventricular muscle from Tg mice (mutated or WT) was washed with an ice-cold EDTA-rigor solution for 0.5 hr followed by an extensive wash with Mg^{2+}-rigor solution to prevent contraction while ATP was being removed. This was followed with wash with Ca^{2+}-rigor solution and homogenization using a Heidolph Silent Crusher S homogenizer for 20 s (with a break to cool after 10 s). We noted that foam formed when a muscle was homogenized in EDTA-rigor solution.

LC1 labeling

LC1was dialyzed against buffer A [50mM KCL and 10mM phosphate buffer (pH 7.0)] and fluorescently labeled by incubating with 5 molar excess of 5-TMRIA for 6 h in buffer A on ice. Unbound dye was eliminated by passing the solution through Sephadex G50 columns. The concentrations of LC1 protein and bound 5-TMRIA were determined to estimate the degree of labeling. Protein concentration was determined by Bradford assay and 5-TMRIA concentration was determined by obtaining the peak absorbance from Varian Eclipse (Palo Alto, CA) spectrometer. The concentration of both the protein and 5-TMRIA dye was found to be the same (10 μM), indicating that the degree of labeling was 100%.

LC1 exchange into myofibrils

Rhodamine labeled LC1 (R-LC1) was incubated with 1 mg/ml of freshly prepared myofibrils in exchange solution [15mM KCl, 5mM EDTA, 5mM DTT, 10mM KH2PO4, 5mM ATP, 1mM TFP, and 10mM imidazole pH 7] [21] for 5 minutes at 30°C. Concentration of R-LC1 was 3 nM unless otherwise specified.

Cross-linking

Polarized intensities during contraction are impossible to record reliably unless muscle shortening is effectively abolished. In our experiments shortening was abolished by cross-linking with water-soluble cross-linker 1-ethyl-3-[3-(dimethylamino)propyl]carbodiimide (EDC)[22, 23]. Briefly: myofibrils (1 mg/ml) were incubated with 20 mM EDC for 20 min at room temperature. The reaction was stopped by adding 20 mM DTT. The lack of shortening was checked by imaging myofibrils by differential contrast microscope, and by fluorescence microscope after labeling myofibrils with 10 nM rhodamine-phalloidin [24]. Cross-linking had no effect on probability distribution measurements [20].

Sample preparation

In contrast to skeletal myofibrils, cardiac myofibrils attached weakly to the glass and were easily displaced by washing. In order to attach them strongly the coverslips were cleaned with 100% ethanol and spin coated with Poly-L-lysine solution (Sigma-Aldrich 0.1%) at

3,000 rpm for 120s using a spincoater P6700 (Specialty Coating Systems, Indianapolis, Indiana).

Rigor force measurements in skinned cardiac papillary muscle fibers

The frozen hearts were thawed and the papillary muscle fibers were isolated. The muscle fibers were then skinned according to Baudenbacher et.al [25]. Briefly, small bundles of fibers were isolated and placed in a pCa 8.0 relaxing solution (10–8 M [Ca^{2+}]free, 1 mM [Mg2+]free, 7 mM EGTA, 2.5 mM MgATP2-, 20 mM MOPS (pH 7.0), 20 mM creatine phosphate, and 15 units/ml creatine phosphokinase, I = 150 mM) containing 1% triton X-100 and 50% glycerol at 4°C for approximately 4–6 hours. Fibers were then transferred to the same solution without triton X-100 and stored at −20°C for up to four days. Mouse muscle fiber bundles with a diameter varying between 65 – 139 mm and ~ 1.3 mm of length were attached to tweezer clips connected to a force transducer. To ensure complete membrane removal and complete access to the myofilament, the fibers were treated with pCa 8.0 containing 1% Triton X-100 for 30 min before the beginning of the experiment. To remove the excess Triton X-100 from the fibers, extensive washing was carried out with pCa 8.0 and then the functional parameters were evaluated. To determine the rigor force under relaxing conditions, the fiber was first extensively rinsed in a pCa 8.0 solution without ATP and then allowed to reach the maximal rigor force in the same solution. However, to determine the rigor force under activating conditions, the fiber was first allowed to contract in pCa 4.0 (in the presence of ATP) and then extensively rinsed in a pCa 4.0 solution without ATP. The fiber was then allowed to reach a plateau and this was considered as the maximal rigor force under activating conditions.

Probability distribution measurements

Alba-FCS (ISS Co, Urbana, IL) confocal system coupled to an Olympus IX 71 microscope was used. The data were collected every 10 μs and was smoothed by binning 1000 points together. The instrument was calibrated and optimized every day with 50 nM solution of rhodamine G. Optimization was carried out until the G-factor (ratio of the orthogonal components) was 1. The excitation was by 635 nm CW laser. Fluorescent light was projected onto dichroic cube (535 SP C107934, Chroma,VT). A polarizer was inserted before the entrance to the microscope to ensure that the exciting light was strictly linearly polarized and vertical on the microscope stage. The laser power was attenuated so as not to illuminate a sample with more than 100 μW. The confocal aperture was 50 μm. The emitted light was split 50/50 by a prism and each component was detected by a separate Avalanche PhotoDiode (APD). The parallel (∥) and perpendicular (⊥) (with respect to the laboratory frame of reference) analyzers were inserted before detectors with the result that APD's of channels 1 and 2 measured the polarized intensities oriented ⊥ and ∥ to the myofibrillar axis, respectively. MFs were always placed with the axis pointing vertically on the microscope stage, i.e. their long axis was always parallel to the direction of polarization. Therefore according to the conventional notation [16]we measure parallel polarization of fluorescence ($PF_{\parallel}$, the subscript denoting direction of excitation polarization with respect to myofibril axis).

Time resolved anisotropy

To test whether rhodamine was rigidly immobilized on the surface of LC1 so that the orientation of the transition dipole of the fluorophore reflects the orientation of the neck of myosin head, we measured the decay of anisotropy of R-LC1 exchanged into skeletal myofibrils. Fluorescence anisotropy was measured by the time-domain technique using FluoTime 200 fluorometer (PicoQuant, Inc.). The excitation was by a 532 -nm laser pulsed diode. The emission was observed through a monochromator at 590 nm with a supporting 590-nm long wave pass filter. The FWHM of pulse response function was 370 ps. Time

resolution was better than 10 ps. The intensity decays were analyzed in terms of a multi-exponential model using FluoFit software (PicoQuant, Inc.). All experiments were performed at ~23°C. The decay of anisotropy [defined as $r=(I_{\parallel}-I_{\perp})/(I_{\parallel}+2I_{\perp})$] of free TMRIA was best fitted by a double exponential curve $r(t)=R_{\infty}+a \cdot \exp(-t/\theta_1) + b \cdot \exp(-t/\theta_2)$ where $R_{\infty} = 0.05$ was the value of anisotropy at infinite time and $\theta_1 = 0.3$ and $\theta_2 = 608.7$ ns were the rotational correlation times. The fast decay dominated the signal (93.1%) - the slow correlation time comprised only 6.9 % of the decay, probably contributed by the aggregates of rhodamine. The decay of R-LC1 in skeletal myofibrils was best fitted by the same double exponential function, but R_{∞} was 0.33, θ1 was 67.7 and θ_2 was 0.9 ns. The slow correlation time comprised 82.1% and the fast correlation time 17.9 % of the decay. The short and long correlation times were most likely due to the rotation of rhodamine moiety on LC1 and to rotation of bound LC1, respectively. The maximum value of anisotropy was 0.384. The high value of initial anisotropy indicates that the absorption and emission dipoles of rhodamine are nearly parallel. Thus the mobile fraction was contributed by the minority of fluorophores and we conclude that LC1 labeling with TMRIA is appropriate for measuring polarization of muscle.

Statistical analysis

It was carried out using Systat (SigmaPlot 11.02 and Origin software (Origin v. 8.5, Northampton, MA). Goodness of fit was assessed by reduced χ^2. Non-linear curve fitting was performed in Origin, which uses the Levenberg-Marquardt algorithm to perform chi-square minimization. The custom software of “velocity" plots (available on request) was written with Labview 2010. Velocities were calculated by taking the difference of consecutive position data points and dividing it by the difference of the time stamps associated with each data point. The plot is the array of velocity data points versus the array of polarization points on an x–y plot. The front panel of Labview program is comprised of a view graph, buttons for initializing the process, storing the data as an excel file, and exporting a graph of the data as a .jpg file. The program was compiled using Labview’s compiler into a stand alone executable.

RESULTS

Global Measurements

We first show that by measuring global parameter (rigor tension) that it is impossible to distinguish between non transgenic (NTg) and Tg-mutated heart preparations. Fig. 2 shows that the rigor tension developed by NTg muscle was not different from average rigor force developed by mutated muscle either in rigor-pCa 8.0 or rigor-pCa 4.0. NTg animals were used as a control for the cardiac skinned papillary muscle fibers, instead of Tg-WT. The difference between the two is that Tg-WT mice carry the human cardiac TnT in the mouse cardiac myofilament background. Previous studies have shown that papillary muscles of both mice (Tg-WT and NTg) develop similar maximal force and have similar Ca^{2+} sensitivity [5, 6].

Mesoscopic measurements

To examine few cross-bridges, rather than to observe a global parameter of muscle, measurements on myofibrils were done as illustrated in Fig. 3. **A** and **B** show typical orthogonal fluorescence intensity images of a single Tg-F110I myofibril from the right ventricle of a mouse in rigor. The image is fainter (**A**) when the emission polarization is perpendicular to the direction of polarization of exciting light than when it is parallel (**B**) indicating that the absorption/emission dipoles of the dye are largely perpendicular to the axis of a myofibril. **C** is the sum of **A** and **B**. D is fluorescence lifetime image. In contrast to skeletal muscle, where nebulin prevents phalloidin from labeling all-but the pointed ends of

actin filaments [26, 27], in the nebulin-free heart muscle the entire I-bands are labeled. The dark areas do not contain actin (H-bands). The red circle in **A** is a 2D projection of the confocal aperture on the image plane. Its diameter is equal to the diameter of the confocal aperture (50 μm) divided by the magnification of the objective (40×). The data is collected from the detection volume (DV) of which the red circle in **A** is a projection (see below).

Number of observed molecules

As explained before the histograms can be meaningfully interpreted only if the data originate from a small number of molecules. To assure that only a small number is observed, native LC1 of myosin was exchanged with a small (3 nM) concentration of labeled LC1. To estimate the number of molecules contributing to the observed fluorescence, we measured signal intensity at decreasing (8.5-1.7 nM) concentrations of the dye. The DV at the focus of the confocal microscope is an ellipsoid of revolution whose waist (1.2 μm) is equal to the diameter of the confocal pinhole ($2\omega_o$=50 μm) divided by the magnification of the objective (40×). The ellipsoid is assumed to have a waist ω_o and height, z_o, equal to the thickness (1 μm) of a typical myofibril. Therefore DV=$4/3\pi\omega_o^2 z_o$ is ~1 μm^3. Knowing the DV and concentration we calculated the number of molecules in the DV. The concentration of 1.7 nM TMRIA corresponds to a single fluorophore. Extrapolation of the signal intensity-concentration curve to 1.7 nM yields number of photons per one fluorophore ≈ 750 counts/s [20].

It is now possible to estimate the number of molecules contributing to the actual signal. The average intensities of ch1 and ch2 for rigor and contracting myofibrils were 14 & 12 counts/10 ms and 50 & 62 counts/10 ms, respectively (not shown). The average was 3500 counts/s. This corresponds to ~5 myosin molecules. It should be emphasized, however, that the exact number of observed cross-bridges does not matter as long as it is mesoscopic, i.e. 5 molecules should give the same result as 10 molecules.

A direct confirmation of this estimation was obtained by calculating the autocorrelation function of orientation fluctuations of contracting muscle.. In this method the number of observed molecules is measured directly by obtaining the autocorrelation function (ACF) of fluctuations of the fluorescence. The value of the autocorrelation function at delay time 0 [G(0)] is equal to the inverse of the number of molecules N contributing to the signal, N=1/G(0)[28, 29]. Fig. 4 shows the typical correlation function of contracting I79N mutated myofibrils. 1/G(0)=0.2 indicating that the number of molecules contributing to fluctuations is 5.

Dispersion of rigor orientations

The rigor distribution of mutated and WT myofibrils differ in width and in the position of the center. A good qualitative illustrations of the differences in the width are “velocity” plots where the "angular velocity" is plotted against PF. The "angular velocity" is defined as the difference of PF at consecutive times divided by 10 ms (hence "angular", because PF is related to the angle of the transition dipole of the dye). Of course it is not actual velocity, which is 0 in rigor. It merely has the units of velocity and is introduced here to create 2D plots of PF. The plots contain the information contained in all 25 experiments done for each mutation. One experiment contains 2000 measurements of PF, i.e. a velocity plot contains 50,000 points. Fig. 5 shows the differences between WT and MUT of rigor myofibrils for each mutation. It is clear that the distribution of polarizations is narrower in WT myofibrils (green) than in MUT myofibrils (red). The meridional lines in Fig. 5 arise because polarization, defined as normalized number of ∥ polarized photons minus number of ⊥ polarized photons, can assume only discrete values. Similarly, the equatorial lines arise because velocity is defined as $\Delta PF/\Delta t$. For each mutation 25 experiments were done.

A difference between WT and MUT myofibrils in rigor was quantified by constructing histograms - plots of the number of events of a given polarization value occurring during 20 s experiment [25]. The histograms were fitted with a Gaussian $y=a\ \exp[-0.5(x-x_o/b)^2]$. The key finding is that the histograms of MUT myofibrils in rigor were more disperse than histograms of WT myofibrils in rigor. The differences between histograms of WT and mutated hearts are shown in representative Figs. 6–8. Each figure shows representative histograms using different mutation. The trend was consistent for each mutation: mutated-rigor MF's were always more disperse and had different center PF than rigor-WT MF's. The quantified difference is shown in Table 1 which lists the center and FWMH for each mutation.

Since FHC mutations are expressed at ~50% level it should be possible to subdivide data into two sets, clustering around different polarizations. This was indeed the case: the data from mutated myofibrils could always be divided into two approximately equal populations, clustering around small and large polarizations. This presumably corresponds to myofibrils carrying a mutation, and myofibrils which were classified as mutated but that carried no mutation. Fig. 9 (top panel) shows the distribution of experimental points in 50,000 measurements on myofibrils carrying F110I mutation. The values of polarizations clearly are clustered around small (green) and large (red) values of PF. The dispersion of rigor histograms was quantified by the value of Full Width at Half Maximum of a single Gaussian fit. Table 2 shows that PF clusters around two distinct values. The differences between FWHM of histograms of WT and the value of high PF of MUT rigor myofibrils were statistically highly significant. This suggest that high PF of MUT myofibrils represents mutated fraction, and low PF of MUT myofibrils represents non-mutated fraction. No clustering occurs in experiments on WT myofibrils (Fig. 9, bottom panel). Similar results were obtained for other mutations.

Skewness and Kurtosis

To characterize data further, we computed skewness and kurtosis of histograms. As mentioned before, a positive skewness means that the tail of the curve points towards positive values of the histogram [30]. A negative skewness means that the tail of the curve points towards the negative values of the histogram. A positive kurtosis is expressed by long tails and lower peaks compared to the Gaussian curves and a negative kurtosis means that the tails are smaller and the peaks are taller than those of Gaussian curves. The values for F110I, R278C and I79N mutations are summarized in Tables 3–5. The differences in skewness between all the heart preparations, whether mutated or not, were not statistically significant. However, the differences in kurtosis between all the TnT mutations in rigor and the values for all other conditions are significant. This was also the case for the muscle carrying A13T mutation in the Regulatory Light Chain (RLC, see Discussion).

DISCUSSION

This report demonstrates that the hypertrophic phenotype associated with FHC mutations in TnT is manifested by large difference in the center and width of distributions of orientation of WT vs. MUT cross-bridges. The increase of FWMHs in MUT myofibrils indicates the loss of order of rigor attachment of the cross-bridges. This effect was clearly visible in the velocity plots of all the data (Fig. 5). The effect was qualitatively demonstrated in Figs. 6–8 which showed that the centers and widths of histograms of mutated myofibrils were dramatically larger than that of WT controls. Table 1 quantified this result. It must be noted that the fact that cross-bridges form improper rigor bonds may not be a direct result of TnT mutations but may be caused by posttranslational modifications status in transgenic animals, MyBP-C phosphorylation etc.

Earlier experiments [5, 6] indicated that maximal force in all TnT mutations was decreased. Our results indicate that mutated muscles suffered a decrease in the number of cross-bridges attached in rigor in a stereo-specific manner. Such attachment is thought to be necessary for force generation [31], and therefore absence of stereo-specificity in rigor suggests that some cross-bridges are unable to contribute to force development. This, in turn, suggests that MUT hearts may be subject to inefficient energy utilization by producing less contractile force than the WT hearts for the same supply of ATP. This would ultimately lead to metabolite accumulation in the mutated myocardium and compromised heart performance, because sustained or progressive demands on the heart can result in a series of compensatory responses including cardiac hypertrophy and myocardial remodeling. In other words, energy expenditure through inefficient energy use would lead to increased turnover of ATP, particularly during stress. From the clinical standpoint, these multilevel changes in cardiac contractility would lead to severe FHC phenotype

The PF values clustered around two distinct values of polarization (Table 2, Fig. 9). This was not surprising because fluorescence is contributed by cross-bridges which interact with actin carrying both WT and MUT TnT. We note that this effect can only be seen in mesoscopic measurements. Conventional measurements, containing contributions from billions of cross-bridges, offer no hope in detecting two populations,

A different way to demonstrate loss of rigor order in cross-bridges of MUT myofibrils is to calculate skewness (S) and kurtosis (K) of histograms. Tables 3–5 show that mutation was associated with increase of both S & K in rigor myofibrils. While S & K by themselves do not prove that the disorder of cross-bridges decreased, they do demonstrate that rigor orientations of cross-bridges in mutated muscle is strikingly different from rigor orientations in WT muscle.

The large dispersion of polarization values observed for mutated myofibrils in rigor could be due either to rotations of the neck region of myosin which do not require hydrolysis of ATP or to the disorder of attachment of myosin to actin carrying mutated TnT. That the observation was made in rigor state does not automatically exclude the possibility that the lever arms rotate. For example, in the model of Coureux, Houdusse and Sweeney, [31] the release of phosphate causes a force-generating conformational change of the bound head. In this low energy state both ADP and actin are bound to myosin head (ADP is bound weakly hence this state is called "weak ADP binding state"). Dissociation of ADP transforms this state to a rigor conformation in which myosin, devoid of hydrolytic products, binds strongly to actin. The global conformation of a cross-bridge in a weak ADP binding state is nearly the same as in rigor, but conformation of LC1 can be completely different. Transition between those states can result in large changes of orientation of LC1 without hydrolysis of ATP. To test this possibility we measured correlation function in rigor, relaxation and contraction. Fig. 10A shows that rigor lever arms do not rotate. Non-zero correlation arises when the fluorescence intensity within the DV changes [28, 32], which in our case arises because transition dipoles of rhodamine change orientation. Conversely, zero correlation arises when the fluorescence intensity within the DV is constant because transition dipoles of rhodamine do not change orientation. Fig. 10A indicates that heads in rigor do not move, i.e. it is impossible that disorder arises from motion of lever arm in rigor. In other words, the myosin heads are stationary and disordered. Conversely, Fig. 10B shows that during contraction the lever arm rotates.

The polarizations observed in mutated hearts in rigor can, in principle, be translated into range of angles that the transition dipole of rhodamine assumes with respect to the myofibrillar axis. However, such translation has not been attempted here because it is critically dependent on the model of arrangement of cross-bridges. For example, in the

model of Tregear & Mendelson [16] which assumes that the cross-bridges are arranged helically along the long axis of muscle and that polarized fluorescence contains α% contribution from random immobilized component, the angle can range from 90° to 5° depending on the value of α [16].

In earlier global studies, fluorescent probes were used to study the breadth of orientation distribution of probes bound to RLC of skeletal muscle myosin. Thus Ling et al. [21] and later Hopkins et al. [4] reported that the breadth of distribution of cross-bridges in skeletal muscle was essentially the same in different physiological states.

Similarly to TnT mutations, 25 experiments on FHC hearts containing A13T mutation in the regulatory light chain revealed a significant increase in the range of polarizations (data not shown). The average skewness of mutated myofibrils in rigor increased by 20% and kurtosis increased by 132% over WT myofibrils in rigor. Thus it is likely that an increase in rigor disorder is a general phenomenon i.e. the stereospecific rigor attachment of force generating myosin cross-bridges is necessary for the normal working of the heart. Any alteration of this important energetic state of the myosin motor could be a triggering factor of cardiomyopathy.

The question remains as to how our findings of the functional deficit at the molecular level explain the diastolic dysfunction? The diastolic dysfunction (decreased ability to relax) may be related to the increased Ca^{2+} affinity to TnC in these mutations (slower off rate of Ca^{2+} from TnC needed for relaxation). Since rigor bridges are known to increase the Ca^{2+} affinity of TnC [33], it is possible that altered rigor bridge binding increases Ca^{2+} affinity and therefore contributes to diastolic dysfunction. We can also speculate that these TnT HCM mutations may have two different components that affect contraction: one component affecting the troponin Ca^{2+} affinity and the other component affecting the maximal force. The component that affects Ca^{2+} affinity would be correlated with diastolic dysfunction since it delays the Ca^{2+} transient [5]. The other component affecting the rigor bonds would be correlated with the decreased maximal force (which is a trend seen in all these three TnT HCM mice).

We have considered five possible artifacts and conclude that all are unlikely:

1. *The fluctuations in orientation are caused by muscle movement, not by cross-bridge rotations.* This is impossible because WT myofibrils were in rigor (i.e. do not move) yet give the small variation in angles (Fig. 6–8). Also, it must be remembered that myofibrils were cross-linked. Even when contraction was induced by adding ATP myofibrils do not shorten. Control experiments using skeletal muscle, where we measured sarcomere length as a function of concentration of cross-linker, showed no shortening in confocal microscope during contraction.
2. *The differences in dispersion of orientations are caused by cross-linking*. This is impossible because all samples were cross-linked, even those (in rigor) that do not require cross-linking. Besides, we have carried out control experiments using skeletal muscle where we measured effect of 20 mM EDC on dispersion of polarization and observed no effect [20].
3. *The effect would be unobservable if the data was fitted by curves different than Gaussian.* This is unlikely because when we fitted some control skeletal data to Lorentzian and Voigt equations, we observed that they are all very similar to the Gaussian fit.
4. *The effect is not due to the loss of stereospecificity of rigor attachments but is due to an increase in disorganization of actin filaments.* This is unlikely because

skewness, kurtosis and center peak positions of histograms are not statistically different for WT and MUT myofibrils in contraction (Tables 3–5). Moreover, both WT and MUT myofibrils give the same narrow distribution of orientations in contraction (data not shown).

5. *Mutations of TnT affect the efficiency of light chain exchange.* This is unlikely because mutations were on a site distant from LC1, the fact that rigor force was unchanged by mutations (Fig. 2) and the fact that our exchange conditions (30°C for 5 min) were mild compared with the conventional ones (37°C for ½ hr).

Highlights
Distribution of orientations of myosin was compared in healthy and hypertrophic hearts>
The distributions were very different in rigor > the hypertrophy is characterized by an increase in disorder of rigor cross-bridges

Glossary

EDC	1-ethyl-3-[3-(dimethylamino)propyl]carbodiimide
Tg	Transgenic
NTg	Non Transgenic
WT	Wild Type
MUT	Mutated
S	Skewness of distribution
K	Kurtosis of distribution
SD	Standard Deviation
FHC	Familial Hypertrophic Cardiomyopathy
TnT	Troponin T
SMD	Single Molecule Detection
LC1	Myosin Essential Light Chain 1
MF	Myofibril
TMRIA	tetramethylrhodamine-5-iodoacetamide dihydroiodide (5-TMRIA) (single isomer)
R-LC1	TMRIA labeled LC1
DV	Detection Volume
HS	Half Sarcomere
RLC	Regulatory Light Chain
ACF	AutoCorrelation Function
APD	Avalanche PhotoDiode
PF	Polarization of Fluorescence
FCS	Fluorescence Correlation Spectroscopy
S	Skewness
K	Kurtosis

Acknowledgments

Supported by the NIH grants R01AR048622 (JB), R01HL090786 (JB and Dr D. Szczesna), NIH grant HL042325(JDP), NIH grant 1K99HL103840-01 and J&E King grant 1KN13-34001 (JRP). AHA grant 10POST3420009 (PM). We thank Dr. R. Fudala for help with MT200 microscope and J. Liang and A. Rojas for the technical assistance with the transgenic animals.

REFERENCES

1. Geeves MA, Holmes KC. The molecular mechanism of muscle contraction. Adv Protein Chem. 2005; 71(24):161–193. [PubMed: 16230112]
2. Sabido-David C, Hopkins SC, Saraswat LD, Lowey S, Goldman YE, Irving M. Orientation changes of fluorescent probes at five sites on the myosin regulatory light chain during contraction of single skeletal muscle fibres. J Mol Biol. 1998; 279(2):387–402. [PubMed: 9642045]
3. Hopkins SC, Sabido-David C, Corrie JE, Irving M, Goldman YE. Fluorescence polarization transients from rhodamine isomers on the myosin regulatory light chain in skeletal muscle fibers. Biophys J. 1998; 74(6):3093–3110. [PubMed: 9635763]
4. Hopkins SC, Sabido-David C, van der Heide UA, Ferguson RE, Brandmeier BD, Dale RE, Kendrick-Jones J, Corrie JE, Trentham DR, Irving M, Goldman YE. Orientation changes of the myosin light chain domain during filament sliding in active and rigor muscle. J Mol Biol. 2002; 318(5):1275–1291. [PubMed: 12083517]
5. Miller T, Szczesna D, Housmans PR, Zhao J, de Freitas F, Gomes AV, Culbreath L, McCue J, Wang Y, Xu Y, Kerrick WG, Potter JD. Abnormal contractile function in transgenic mice expressing a familial hypertrophic cardiomyopathy-linked troponin T (I79N) mutation. J Biol Chem. 2001; 276(6):3743–3755. Epub 2000 Nov 1. [PubMed: 11060294]
6. Hernandez OM, Szczesna-Cordary D, Knollmann BC, Miller T, Bell M, Zhao J, Sirenko SG, Diaz Z, Guzman G, Xu Y, Wang Y, Kerrick WG, Potter JD. F110I and R278C troponin T mutations that cause familial hypertrophic cardiomyopathy affect muscle contraction in transgenic mice and reconstituted human cardiac fibers. J Biol Chem. 2005; 280(44):37183–37194. [PubMed: 16115869]
7. Gomes AV, Potter JD. Molecular and cellular aspects of troponin cardiomyopathies. Ann N Y Acad Sci. 2004; 1015:214–224. [PubMed: 15201162]
8. Chase PB. Tropomyosin in the groove? Molecular insights into an inherited myopathy. J Physiol. 2007; 581(Pt 3):889. [PubMed: 17525111]
9. Mathur MC, Kobayashi T, Chalovich JM. Some cardiomyopathy-causing troponin I mutations stabilize a functional intermediate actin state. Biophys J. 2009; 96(6):2237–2244. [PubMed: 19289050]
10. Willott RH, Gomes AV, Chang AN, Parvatiyar MS, Pinto JR, Potter JD. Mutations in Troponin that cause HCM, DCM AND RCM: what can we learn about thin filament function? J Mol Cell Cardiol. 2010; 48(5):882–892. [PubMed: 19914256]
11. Wen Y, Xu Y, Wang Y, Pinto JR, Potter JD, Kerrick WG. Functional effects of a restrictive-cardiomyopathy-linked cardiac troponin I mutation (R145W) in transgenic mice. J Mol Biol. 2009; 392(5):1158–1167. [PubMed: 19651143]
12. Qian H, Saffarian S, Elson EL. Concentration fluctuations in a mesoscopic oscillating chemical reaction system. Proc Natl Acad Sci U S A. 2002; 99(16):10376–10381. Epub 2002 Jul 17. [PubMed: 12124397]
13. Dos Remedios CG, Millikan RG, Morales MF. Polarization of tryptophan fluorescence from single striated muscle fibers. A molecular probe of contractile state. J. Gen. Physiol. 1972; 59:103–120. [PubMed: 4332133]
14. Dos Remedios CG, Yount RG, Morales MF. Individual states in the cycle of muscle contraction. Proc Natl Acad Sci U S A. 1972; 69:2542–2546. [PubMed: 4341699]
15. Nihei T, Mendelson RA, Botts J. Use of fluorescence polarization to observe changes in attitude of S1 moieties in muscle fibers. Biophys. J. 1974; 14:236–242. [PubMed: 4132695]
16. Tregear RT, Mendelson RA. Polarization from a helix of fluorophores and its relation to that obtained from muscle. Biophys. J. 1975; 15:455–467. [PubMed: 19211017]

17. Morales MF. Calculation of the polarized fluorescence from a labeled muscle fiber. Proc Nat Acad Sci USA. 1984; 81:145–149. [PubMed: 6582471]

18. Burghardt TP, Ajtai K. Following the rotational trajectory of the principal hydrodynamic frame of a protein using multiple probes. Biochemistry. 1994; 33:5376–5381. [PubMed: 8180160]

19. Muthu P, Mettikolla P, Calander N, Luchowski R, Gryczynski I, Gryczynski I, Szczesna-Cordary D, Borejdo J. Single Molecule Kinetics in the Familial Hypertrophic Cardiomyopathy D166V Mutant Mouse Heart. Journal of Molecular and Cellular Cardiology. 2009; 48(6):1264–1271.

20. Midde, k; Luchowski, R.; Das, HK.; Fedorick, J.; Dumka, V.; Gryczynski, I.; Gryczynski, Z.; Borejdo, J. Evidence for pre-and post-power stroke of cross-bridges of contracting skeletal myofibrils. Biophys. J. 2011; 100(4):1024–1033. [PubMed: 21320447]

21. Ling N, Shrimpton C, Sleep J, Kendrick-Jones J, Irving M. Fluorescent probes of the orientation of myosin regulatory light chains in relaxed, rigor, and contracting muscle. Biophys. J. 1996; 70:1836–1846. [PubMed: 8785344]

22. Herrmann C, Lionne C, Travers F, Barman T. Correlation of ActoS1, myofibrillar, and muscle fiber ATPases. Biochemistry. 1994; 33(14):4148–4154. [PubMed: 8155632]

23. Tsaturyan AK, Bershitsky SY, Burns R, Ferenczi MA. Structural changes in the actin-myosin cross-bridges associated with force generation induced by temperature jump in permeabilized frog muscle fibers. Biophys J. 1999; 77(1):354–372. [PubMed: 10388763]

24. Borejdo J, Muthu P, Talent J, Akopova I, Burghardt TP. Rotation of Actin Monomers during Isometric Contraction of Skeletal Muscle. J. Biomed. Optics. 2007; 12(1) 014013.

25. Baudenbacher F, Schober T, Pinto JR, Sidorov VY, Hilliard F, Solaro RJ, Potter JD, Knollmann BC. Myofilament Ca2+ sensitization causes susceptibility to cardiac arrhythmia in mice. J Clin Invest. 2008; 118(12):3893–3903. [PubMed: 19033660]

26. Szczesna D, Lehrer SS. The binding of fluorescent phallotoxins to actin in myofibrils. J Muscle Res Cell Motil. 1993; 14(6):594–597. [PubMed: 8126219]

27. Ao X, Lehrer SS. Phalloidin unzips nebulin from thin filaments in skeletal myofibrils. J Cell Sci. 1995; 108(Pt 11):3397–3403. [PubMed: 8586652]

28. Magde D, Elson EL, Webb WW. Fluorescence correlation spectroscopy. II. An experimental realization. Biopolymers. 1974; 13(1):29–61. [PubMed: 4818131]

29. Elson, EL. Introduction to FCS. In: Gryczynski, Z., editor. Short Course on Cellular and Molecular Fluorescence. Vol. Vol. 2. Fort Worth: UNT; 2007. p. 1-10.

30. Borejdo J, Szczesna-Cordary D, Muthu P, Calander N. Familial Hypertrophic Cardiomyopathy Can Be Characterized by a Specific Pattern of Orientation Fluctuations of Actin Molecules. Biochemistry. 2010; 49:5269–5277. [PubMed: 20509708]

31. Coureux PD, Sweeney HL, Houdusse A. Three myosin V structures delineate essential features of chemo-mechanical transduction. Embo J. 2004; 23(23):4527–4537. [PubMed: 15510214]

32. Elson EL, Magde D. Fluorescence Correlation Spectroscopy: Coceptual Basis and Theory. Biopolymers. 1974; 13:1–28.

33. Guth K, Potter JD. Effect of rigor and cycling cross-bridges on the structure of troponin C and on the Ca2+ affinity of the Ca2+-specific regulatory sites in skinned rabbit psoas fibers. J Biol Chem. 1987; 262(28):13627–13635. [PubMed: 3654633]

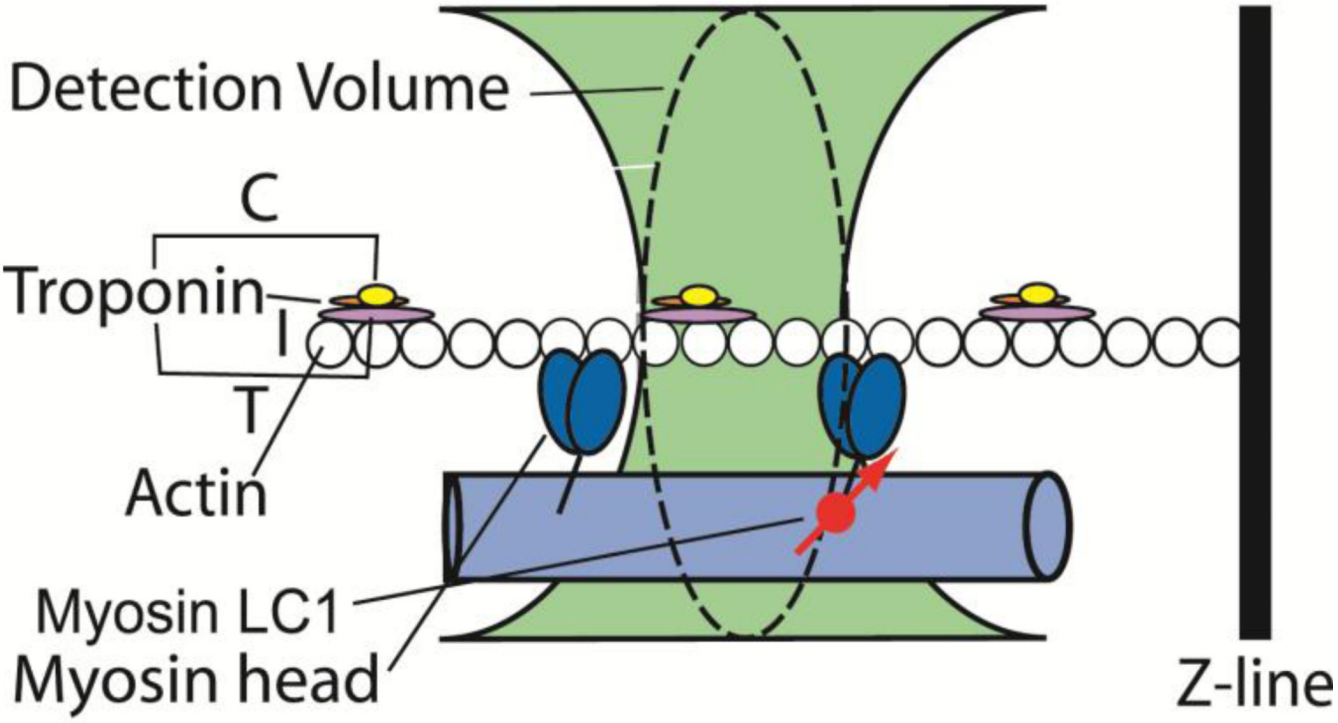

Fig. 1.

Origin of fluctuations. Small fraction of myosin carries fluorescently labeled LC1 (red circle).The transition dipole of the fluorophore is shown as a red arrow. The C,I and T subunits of troponin are shown in yellow, orange and violet, respectively. Rotations of myosin cross-bridges change the orientation of a transition dipole of rhodamine and cause fluctuations of polarized intensity. We measure fluctuations by recording the parallel (∥) and perpendicular (⊥) components of fluorescent intensity of light emitted by a cross-bridge-bound fluorophore.

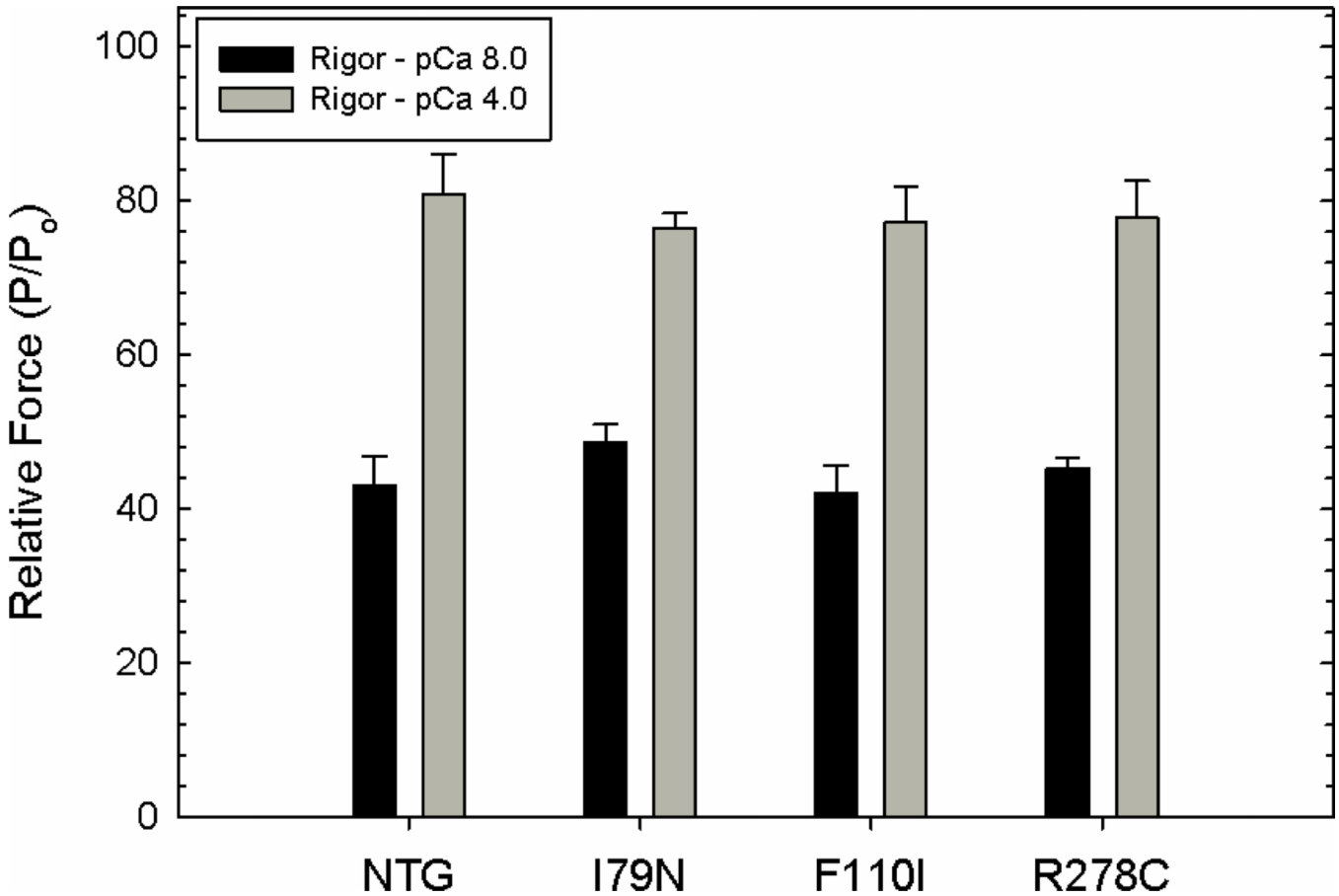

Fig. 2.

Rigor-force measurements under relaxing (pCa 8) and activating (pCa 4) conditions. Relative force in NTG and Tg-mutated skinned cardiac papillary muscle fibers. Relative force = Maximal force developed by the fiber under rigor conditions (P) / Initial maximal force measured under Ca^{2+}-activating conditions (Po). Data is shown as mean ± S.E. , n =6. As a control for the cardiac skinned papillary muscle fibers, non transgenic (NTG) were used instead of Tg-WT mice due to lack of animals. The difference between the two is that Tg-WT mice carry the human cardiac TnT in the mouse cardiac myofilament background. Previous studies have shown that both mice develop similar maximal force and have similar Ca^{2+} sensitivity [5, 6].

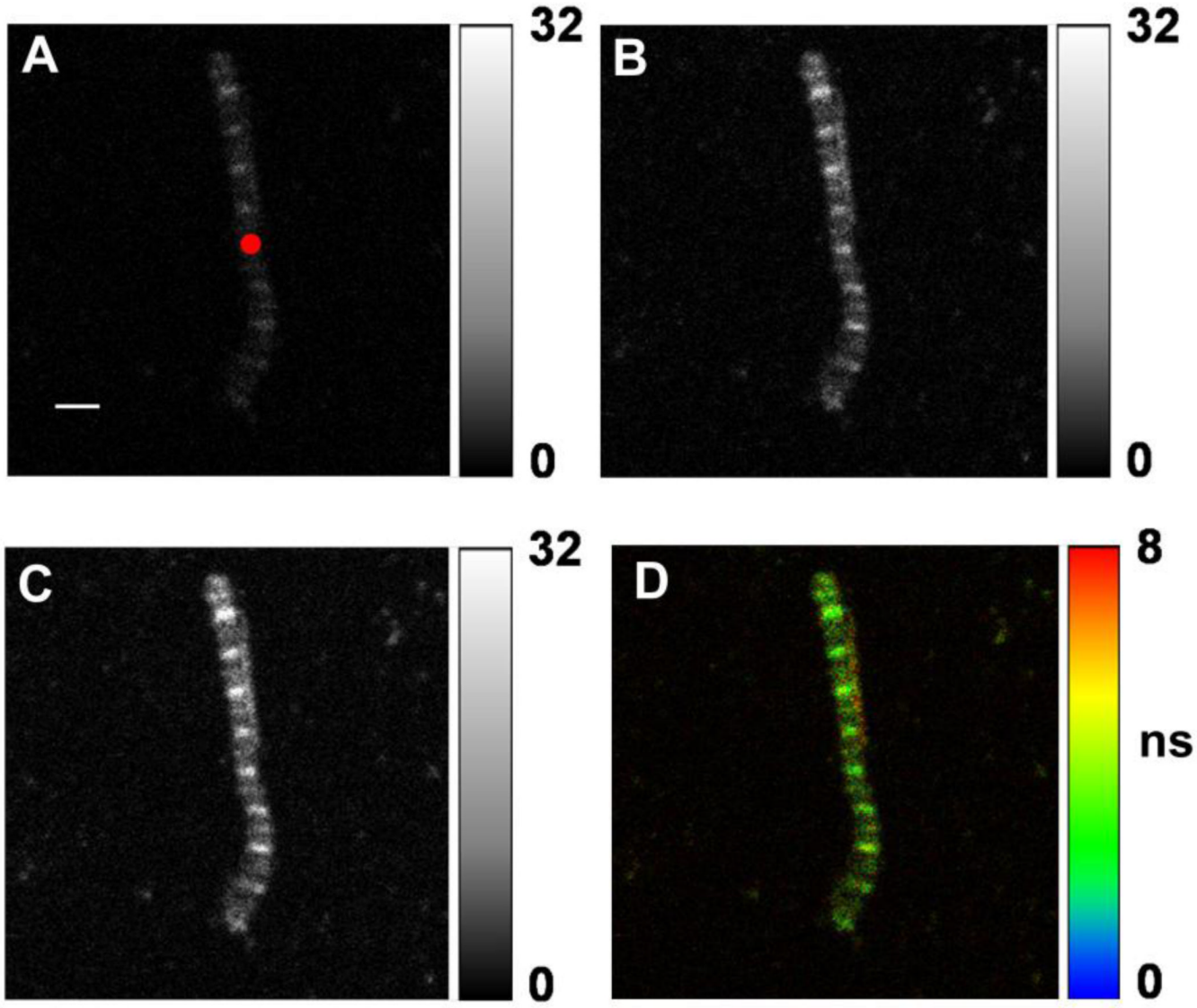

Fig. 3.

Images of a rigor myofibril with F110T mutation in TnT. Native LC1's of cardiac myofibrils exchanged with 3 nM of R-LC1. The red circle in A is the projection of the confocal aperture on the sample plane (diameter 1.2 μm). The numbers at right of A–C indicate the B/W scale with 0 corresponding to black and 255 to white. Polarization of laser is vertical. A-emission polarization horizontal; B-emission polarization vertical; C-both emissions together. D is the lifetime image with blue corresponding to 0 and red to 8 ns. Bar in A is 2 μm, sarcomere length= 1.7 μm. The images are indistinguishable from WT myofibrils. Images acquired with the PicoQuant Micro Time 200 confocal lifetime microscope. Excitation with a 470 nm pulse of light, emission through LP500 filter.

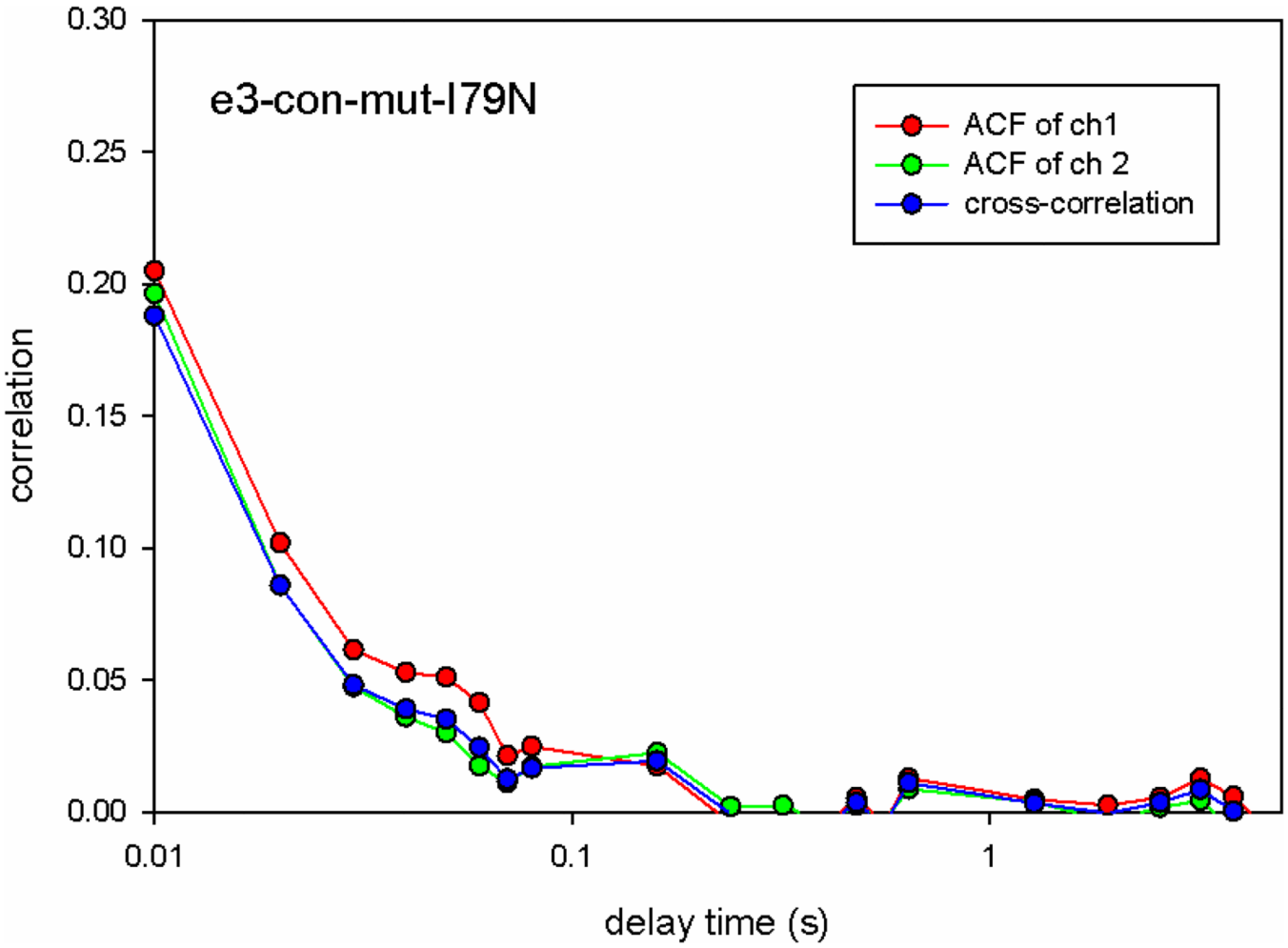

Fig. 4.

Correlation function G of contracting myofibrils. Red, green and blue curves are autocorrelation functions of ch1 (*perpendicular*), ch2 (parallel) and cross-correlation function of ch1 × ch2, respectively. They are essentially the same, all indicating that N=1/G(0)=5.

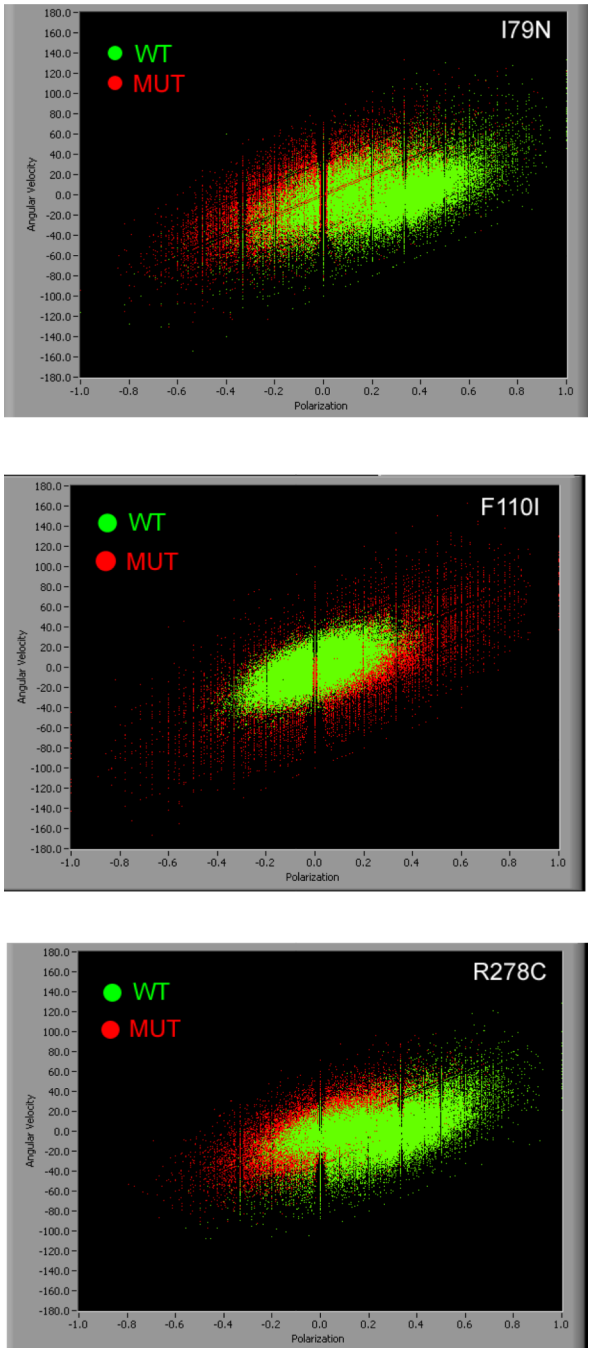

Fig. 5.
Polarized fluorescence plotted against angular velocity of 50,000 measurements of WT (green) and MUT (red) rigor myofibrils. Top: I79N, middle: F110I, bottom: R278C myofibrils.

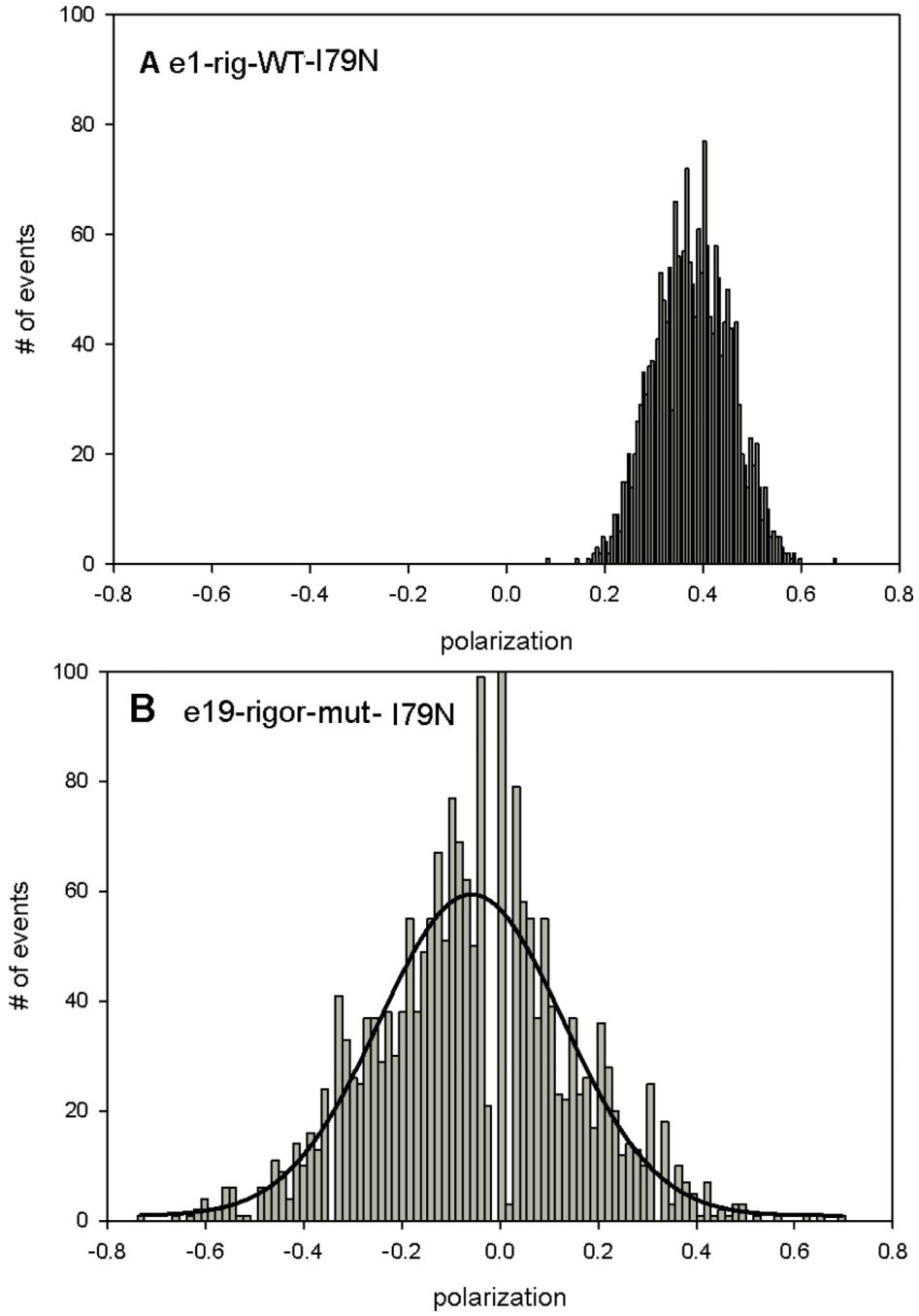

Fig. 6.

Typical histograms of polarized fluorescence of rigor-WT (A) and rigor-MT (B) myofibrils from ventricular muscle with I79N mutation in TnT. The solid line is the best fit to the Gaussian 3 parameter function $y=a\cdot\exp[(-0.(5(x-x_0)/b)^2]$. Notice that the same muscle was used in A and B.

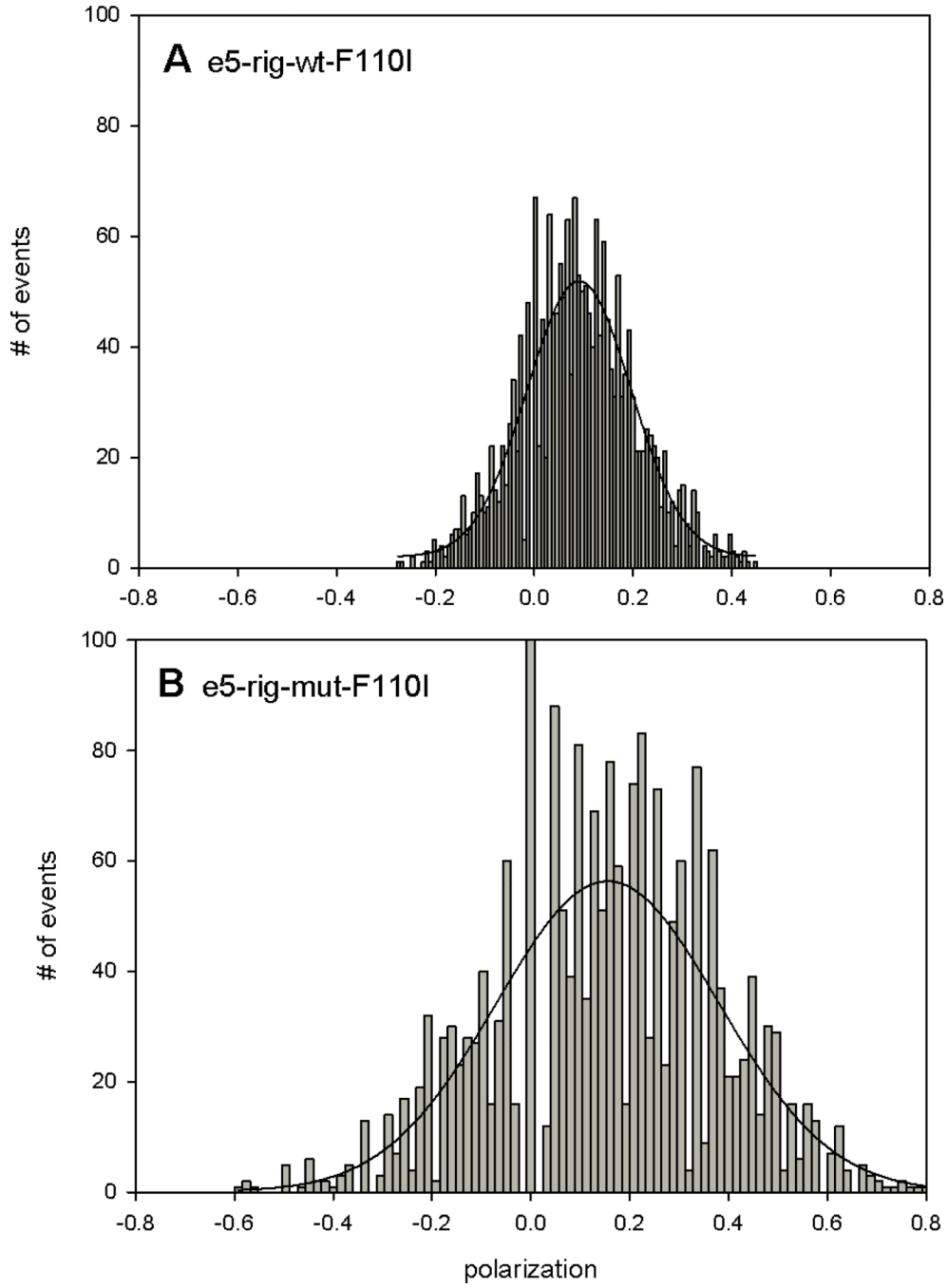

Fig. 7.

Typical histograms of polarized fluorescence of rigor WT (A) and rigor mutated (B) myofibrils from ventricular muscle with F110I mutation in TnT. The solid line is the best fit to the Gaussian 3 parameter function $y=a\cdot\exp[(-0.(5(x-x_o)/b)^2]$. The same muscle was used in A and B.

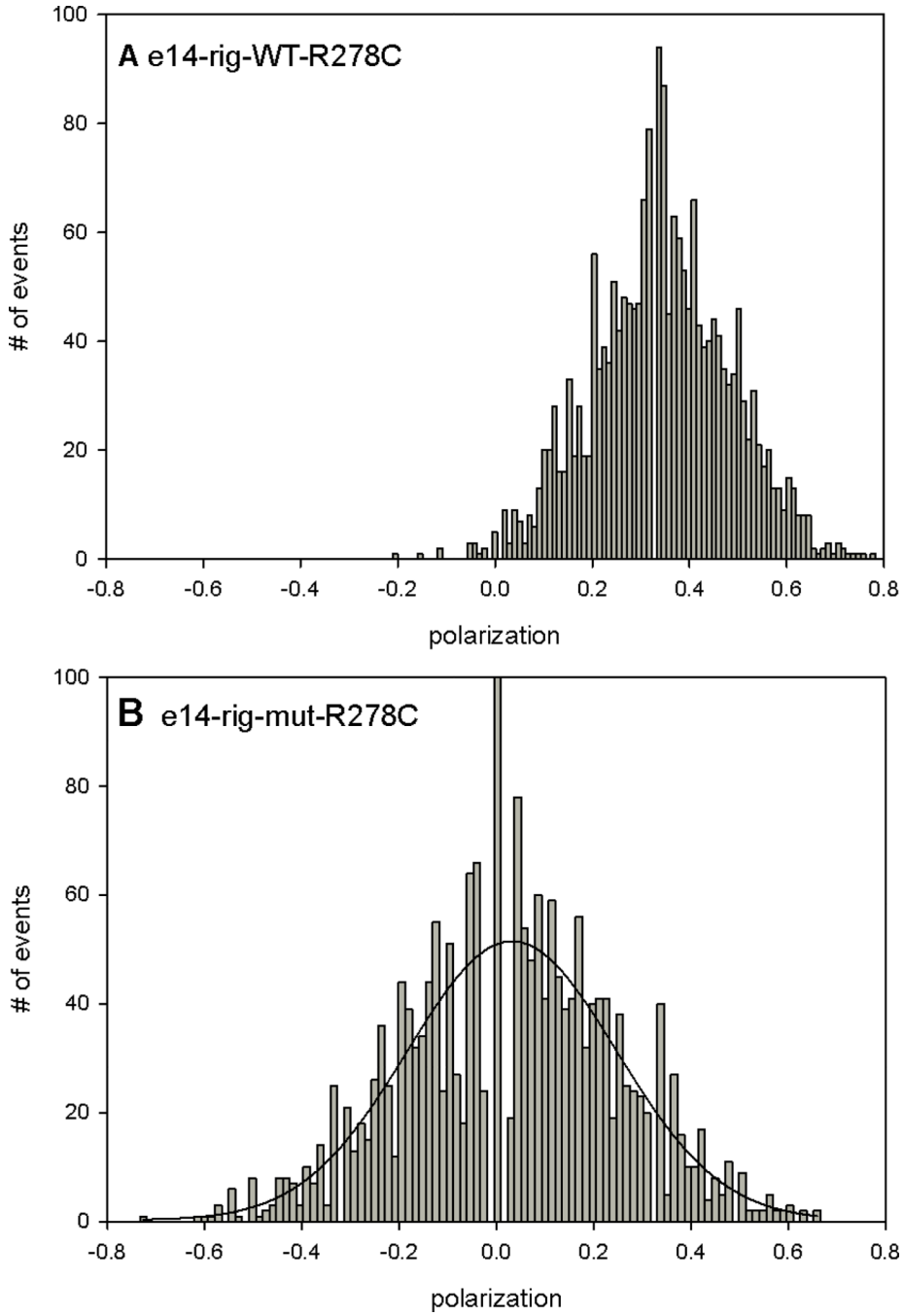

Fig. 8.

Typical histograms of polarized fluorescence of rigor-WT (A) and rigor-MT (B) myofibrils from ventricular muscle with R278C mutation in TnT. The solid line is the best fit to the Gaussian 3 parameter function $y=a\cdot\exp[(-0.(5(x-x_0)/b)^2]$. The same muscle was used in A and B.

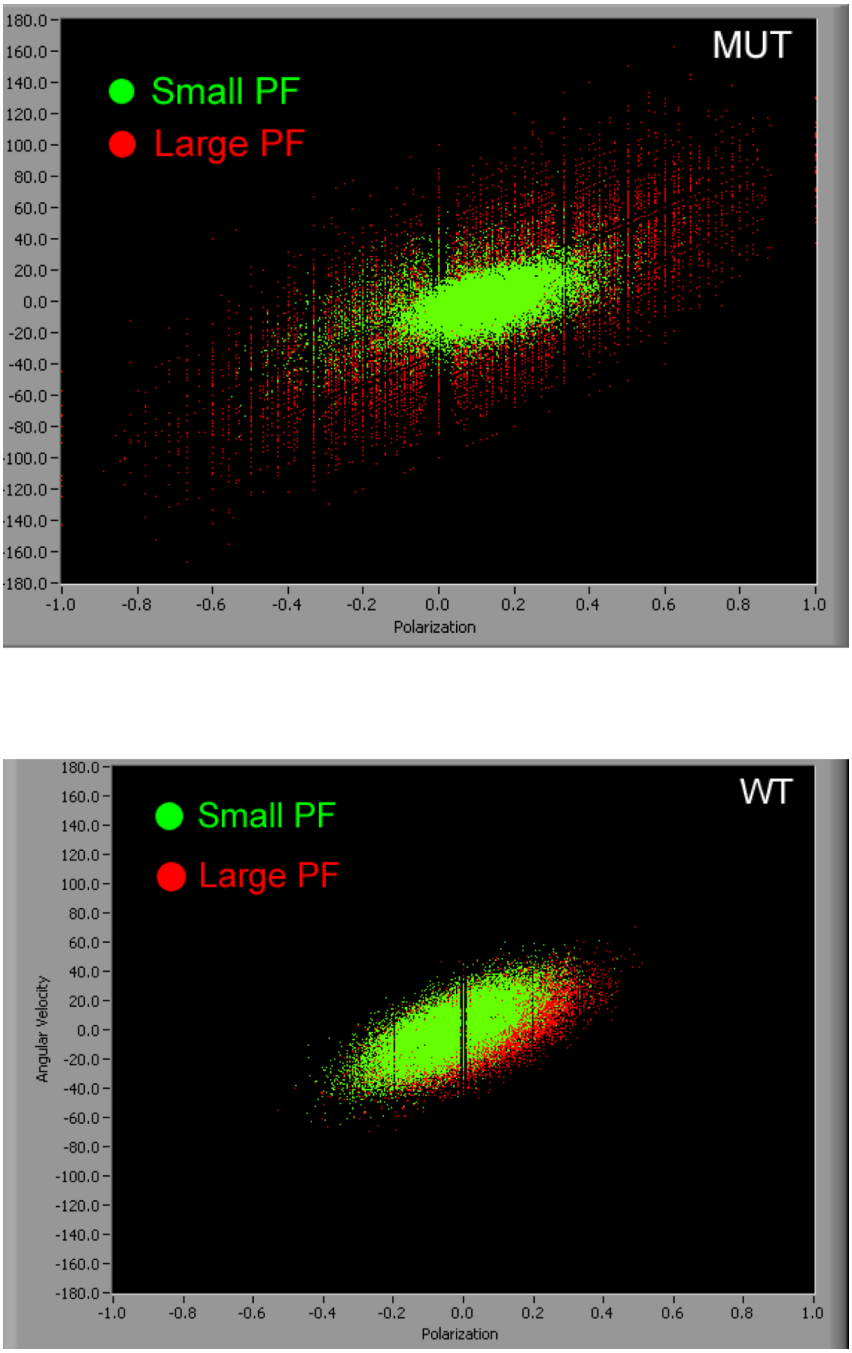

Fig. 9.

Top panel: Polarized fluorescence plotted against angular velocity of 24,000 measurements of mutated myofibrils which had small values of polarization (green) and 26,000 measurements of mutated myofibrils which had large values of polarization (red). Bottom panel: as above, but for WT myofibrils.

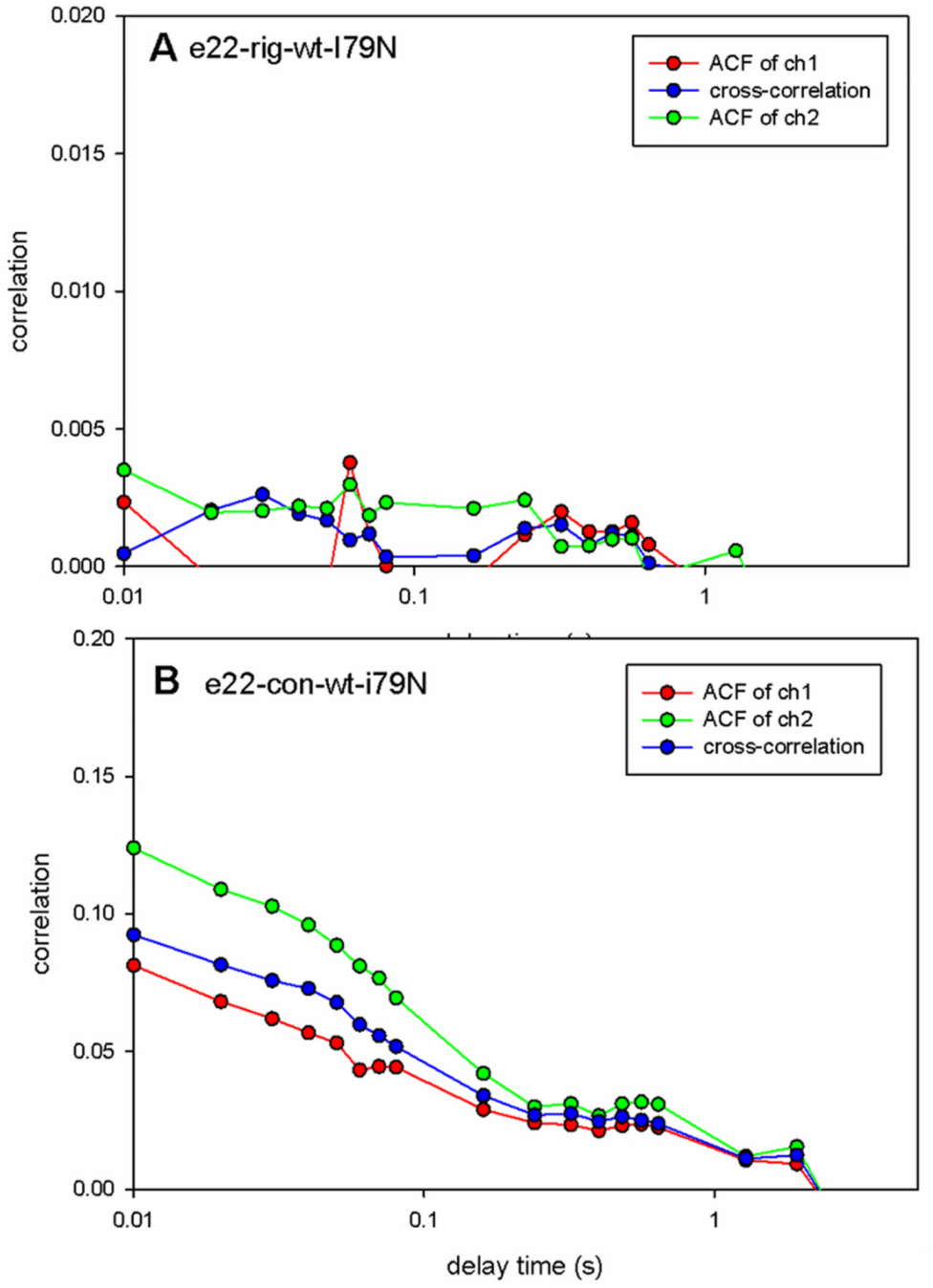

Fig. 10.

Correlation functions of rigor (A) and contracting (B) myofibrils. Note that the vertical scale in A is 10 times smaller than in B, i.e. correlation is nearly zero: cross-bridges do not rotate. Muscle with I79N mutation. Red: ACF of *perpendicular component of polarization signal, green:* parallel component, blue: cross-correlation function of parallel and perpendicular components.

Table 1

Distribution of rigor polarizations can be characterized by FWMH and position of the Gaussian peak.

Sample	FWHM±SD	Peak±SD
I79N-WT	0.29±0.10	0.26±0.14
I79N-MUT	0.32±0.09	0.04±0.14
F110I-WT	0.22±0.01	0.00±0.04
F110I-MUT	0.34±0.18	0.10±0.08
R278C-WT	0.20±0.07	0.26±0.12
R278C-MUT	0.28±0.06	0.04±0.09

Table 2

Rigor polarizations of mutated myofibrils showing that the values cluster around low and high values.

Sample	FWHM
Average for WT	0.25±0.05
F110I-MUT-lowPF	0.14±0.02
F110I-MUT-highPF	0.48±0.09
R278-MUT-lowPF	0.29±0.03
R278C-MUT-highPF	0.31±0.06
I79N-MUT-lowPF	0.22±0.03
I79N-MUT-highPF	0.39±0.06

Table 3

Mean and Standard Deviation of Skewness and Kurtosis of 25 heart muscles expressing I79N mutation. Con indicates contraction.

Sample	Skewness±SD	Kurtosis±SD	Peak±SD
I79N-WT-rigor	1.24±0.55	1.48±2.95	0.26±0.14
I79N-MUT-rigor	1.44±0.58	2.71±3.40	0.04±0.14
I79N-WT-con	1.06±0.31	0.25±1.22	0.28±0.03
I79N-MUT-con	0.85±0.21	−0.49±0.69	0.21±0.08

Table 4

Mean and Standard Deviation of Skewness and Kurtosis of 25 heart muscles expressing F110I LV mutation.

Sample	Skewness±SD	Kurtosis±SD	Peak±SD
F110I-WT-rigor	1.10±0.15	0.51±0.70	0.00±0.04
F110I-MUT-rigor	1.64±0.09	4.49±7.02	0.10±0.08
F110I-WT-con	0.87±0.13	−0.60±0.29	0.15±0.05
F110I-MUT-con	1.04±0.37	0.09±1.48	0.16±0.06

Table 5

Mean and Standard Deviation of Skewness and Kurtosis of 25 heart muscles expressing R278C mutation.

Sample	Skewness±SD	Kurtosis±SD	Peak±SD
R278C-WT-rigor	0.99±0.32	0.19±1.19	0.26±0.12
R278C-MUT-rigor	1.23±0.48	1.66±3.41	0.04±0.09
R278-WT-con	0.70±0.16	−0.80±0.28	0.13±0.18
R278C-MUT-con	0.86±0.25	−0.33±1.08	0.14±0.14